A New Rhodamine B-based Fluorescent Probe for pH Detection and Bioimaging under Strong Acidic Conditions

Quan Yang,[†] Jingrong Zou,[†,‡] Sridhar Chirumarry,[†,§] Chang Huo,[†] Linlin Tang,[†,‡] Fang Zhang,[†,‡] Yi Xiang,[†] Hua Zuo,[†,‡] Dong-Soo Shin,[†,§,*] and Xiang Peng[†,*]

[†]*Department of Cardiology, The Fourth People's Hospital of Sichuan Province, Chengdu 610-016, China. *E-mail: dsshin@changwon.ac.kr; 1070715337@qq.com*
[‡]*College of Pharmaceutical Sciences, Southwest University, Chongqing 400715, China*
[§]*Department of Chemistry, Changwon National University, Changwon 641-773, South Korea*
Received April 4, 2016, Accepted July 7, 2016, Published online September 7, 2016

A new pH-sensitive rhodamine derivative was designed and synthesized using coupling reaction of rhodamine hydrazine with commercially available 3-bromo-4-hydroxybenzaldehyde, and characterized *via* NMR, HRMS, UV and fluorescent spectra. The obtained probe was marked with yellow fluorescence under neutral condition and pink in strongly acidic media. It has high quantum yields, is not susceptible to metal interference, and has high penetration ability for cell membrane and also further applicable in bioimaging.

Keywords: pH-sensitive probe, Rhodamine B derivative, Fluorescence, Bioimaging, Acidic condition

Introduction

Monitoring pH change is an essential technology required in chemical, biological and industrial fields, such as chemical and biological analyses,[1,2] environmental protection,[1,3] and chemical process control.[4] Although, the potentiometric method using a glass electrode is most widely used for pH determination, the glass pH electrode suffers from limitations including the requirement for a reference electrode,[3] frequent calibration, the susceptibility to electrical interference,[4] instability, possible damage and being too bulky for many *in vivo* use.[5] In recent years, the optical pH-sensing technique based on the absorption or emission of certain dyes has gained increasing attention because it offers many advantages over the potentiometric method and nuclear magnetic resonance (NMR), such as rapid response time, real time sensing,[3,6] electrical safety,[1] a wide selection of available indicator dyes,[7–9] particularly high selectivity and sensitivity. New fluorescent pH chemosensors are also continually developed and commercially available, such as small molecules derived from aminophthalimide,[4] cyanine,[10] BODIPY dyes,[11,12] benzoxanthenes,[13] fluorescein,[14] and so on,[15–17] but most of them are associated with biotechnological applications and thus concerns on pH sensors gained attention for the physiological range.[14,18–20] Relatively less attention has been paid to fluorescent probes, which are promising candidates for pH detection in the lower pH region (pH < 4).[3] In fact, some media such as those found in the human stomach[21,22] or environmental water[3] are strongly acidic and certain microorganisms, including *Helicobacter pylori* and "acidophiles" favor such harsh conditions, therefore it is necessary to develop chemosensors for indicating pH levels of these highly acidic media.

It remains a challenge to develop fluorescent sensors that respond to extreme acidity because of the weak fluorescence and chemical instability of fluorescein or coumarin under strongly acidic conditions.[23] Nevertheless, based on the changes in spectroscopic phenomena, such as absorption and fluorescence due to the reversible changes in the indicator's spirocyclic structure induced by pH, rhodamine B derivatives serve as excellent "off-on" fluorescent probes.[24–26] Given that the fascinating structure and unparalleled photophysical properties, such as high quantum yields, large Stokes shifts, large extinction coefficients, and great photostability,[18] some lower pH-sensitive rhodamine derivatives were reported.[27–29]

Herein, we synthesized a novel pH-sensitive rhodamine derivative using rhodamine hydrazine and commercially available 3-bromo-4-hydroxybenzaldehyde. A conjugated substituted styryl moiety was introduced to rhodamine core and the obtained probe exhibits strong yellow and pink fluorescence under neutral and acidic conditions, respectively. In comparison to the reported results related to highly acidic sensors,[30] the new probe has higher quantum yields, is less susceptible to metal interference, and has high penetration ability for cell membrane.

Experimental

Chemicals and Apparatus. Deionized water was used throughout the experiment. All the reagents were obtained from commercial sources and used without further purification. The metal salts used were $Al(NO_3)_3{\cdot}9H_2O$, $Ba(NO_3)_2$, $Ca(NO_3)_2{\cdot}4H_2O$, $Co(NO_3)_2{\cdot}6H_2O$, $CsNO_3$, $Cu(NO_3)_2{\cdot}3H_2O$, $Fe(NO_3)_3{\cdot}9H_2O$, $Hg(NO_3)_2$, KNO_3, $LiNO_3$, $Mg(NO_3)_2{\cdot}6H_2O$, $Mn(NO_3)_2$, $NaNO_3$, $Ni(NO_3)_2{\cdot}6H_2O$ and $Zn(NO_3)_2{\cdot}6H_2O$. Britton–Robinson (B–R) buffer was

prepared by mixing 40 mM acetic acid, 40 mM boric acid, and 40 mM phosphoric acid. Dilute hydrochloric acid or sodium hydroxide was used for tuning pH values. Melting point (uncorrected) was determined on a micromelting point apparatus (Shanghai Shenguang Instrument Co. Ltd., Shanghai, China). ^{1}H and ^{13}C NMR (nuclear magnetic resonance) spectra (at 400 MHz and 100 MHz, respectively) were recorded in $CDCl_3$ with tetramethylsilane as internal reference on a Bruker Advance500 FT spectrometer. Chemical shifts were reported in parts per million. IR spectra were recorded on a FT-IR-6300 (JASCO, Tokyo, Japan) and Mass spectra (MS) were measured by the ESI method on an Agilent 6510 Q-TOF mass spectrometer. Aluminum oxide (100–200 mesh) was used for flash column chromatography. All reactions were monitored by TLC (thin-layer chromatography) using 0.25 mm silica gel plates with UV indicator (Shanghai Jiapeng Technology Co., Ltd., Shanghai, China). UV–vis spectra were recorded on a UV-2550 spectrometry (Hitachi, Tokyo, Japan). Fluorescent measurements were recorded on an F-4500 FL spectrophotometer (Hitachi). The pH measurements were performed on a PHS-3C digital pH meter (Mettler Toledo, Greifensee, Switzerland). Images of *Escherichia coli* cells were captured with a laser confocal microscope (Carl Zeiss LSM-700, Oberkochen, Germany).

Synthesis of Probe L. The synthetic route of **L** is shown in Scheme 1. The reaction of $NH_2NH_2{\cdot}H_2O$ (0.050 mmol, 2.0 equiv) with rhodamine-B **1** (0.025 mmol, 1.0 equiv) in refluxed ethanol (50 mL) led to the formation of rhodamine hydrazide **2**.[30] The solution of rhodamine hydrazide **2** (0.025 mmol, 1.0 equiv) and 3-bromo-4-hydroxy benzaldehyde (0.100 mmol, 4.0 equiv) in ethanol (20 mL) was then refluxed for 16 h and monitored by TLC. After the completion of the reaction, the mixture was evaporated to dryness and 30 mL water was added to the residue. The product was extracted by ethyl acetate (20 mL) from water for three times and further recrystallization from ethyl acetate afforded the target probe. The probe **L** was obtained as a white solid in 85% yield and the structure was determined by ^{1}H NMR, ^{13}C NMR, IR, and HRMS spectra (Figures S1, S3–S5, Supporting Information).

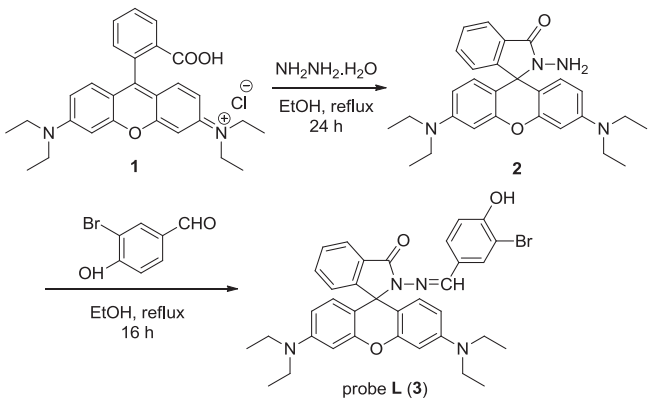

Scheme 1. The synthetic route of probe **L**.

2-((3-Bromo-4-hydroxybenzylidene)amino)-3′,6′-bis (diethylamino)spiro[isoindoline-1,9′-xanthen]-3-one (**3**): mp 225–228°C. ^{1}H NMR (400 MHz, $CDCl_3$) δ 8.37 (s, 1H), 7.99 (d, J = 6.8 Hz, 1H), 7.66 (s, 1H), 7.57–7.34 (m, 3H), 7.10 (d, J = 6.8 Hz, 1H), 6.96 (d, J = 8.4 Hz, 1H), 6.51 (d, J = 8.8 Hz, 2H), 6.44 (s, 2H), 6.24 (d, J = 7.6 Hz, 2H), 6.06 (s, 1H), 3.32 (dd, J = 13.4, 6.5 Hz, 8H), 1.16 (t, J = 6.8 Hz,12H). ^{13}C NMR (101 MHz, $CDCl_3$) δ 153.5, 153.0, 151.9, 148.9, 145.1, 133.3, 131.0, 129.6, 129.0, 128.5, 128.2, 127.9, 123.7, 123.4, 115.8, 110.4, 108.0, 105.8, 97.9, 65.9, 44.3, 12.6. IR(KBr): ν_{max} 3437, 3128, 2968, 1685, 1610, 1519, 1371, 1280, 1217, 1109, 810, 769, 696 cm^{-1}. HRESIMS *m/z*: calcd for $C_{35}H_{35}BrN_4O_3^+$: 638.1893, found: 639.1957 $[M + H]^+$; $C_{35}H_{35}BrN_4O_3^{2+}$: 640.1893, found: 641.1878 $[M + 2 + H]^+$.

Bacteria Culture and Imaging. *Escherichia coli* was incubated at 37°C in Luria–Bertani (LB) culture (tryptone 10 g/L, yeast extract 5 g/L, NaCl 10 g/L) in a table concentrator (AO HUA, ZD-85, Changzhou, China) at 180 rpm for 5 h, and the culture was centrifuged (Heal Force TGL-16M, Changsha, China) in 10 mL Eppendorf tubes at 10 000 rpm for 5 min. The sediment was then resuspended in B–R buffer at pH 1.75, 2.30, and 4.83, respectively. The pH probe dissolved in ethanol was added into each buffer, with a final concentration at 25 μM after resuspension. *Escherichia coli* cells with the probe were then incubated in the table concentrator as mentioned above for 30 min, washed by deionized water and smeared on slides. The color changes of *E. coli* cells were observed at the wavelength of 555 nm under laser confocal microscopy.

Results and Discussion

Spectroscopic Properties and Optical Responses to pH. Probe **L** showed high sensitivity towards strong acidic condition, which is clarified in Figure 1. The fluorescence intensity of probe **L** slightly increased with decreasing pH value from 11.12 to 4.00, and it began to dramatically rise under strongly acidic condition (pH < 3.06) and the maximum intensity appeared at 577 nm when the pH reached 1.75. It is assumed that probe **L** was present in the form of spirolactam structure at high pH value and the ring quickly opened to form a conjugated form under strong acidic condition, which was confirmed by ^{1}H NMR analysis.[31,32] The titration of probe **L** with 2.0 equiv trifluoroacetic acid (TFA) in solution of $CDCl_3$ showed the down-field shifts for the signals of hydrogen atoms of the 2-bromo-4-(1-iminoethyl)phenol and xanthene moiety of rhodamine in ^{1}H NMR. These shifts due to the change of the electron cloud density of rhodamine Schiff-base group were assumed to be caused by proton promoted conversion of spirolactam structure (nonfluorescent) to a conjugated ring-opened form (fluorescent) under strong acidic condition (Figure S2).

The fluorescence intensity at 577 nm decreased sharply when pH value increased from 1.75 to 4.00 according to

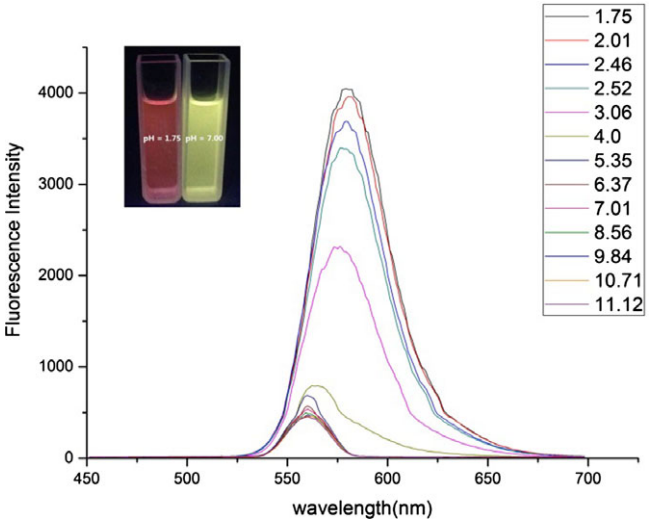

Figure 1. The fluorescence emission spectrum of **L** (25 μM) in solution (B–R buffer-EtOH, v/v = 1:1) with different pH. The inset showed the fluorescence color of **L** with at pH 1.75 (left) and 7.00 (right) (excitation wavelength: λ_{ex} = 560 nm).

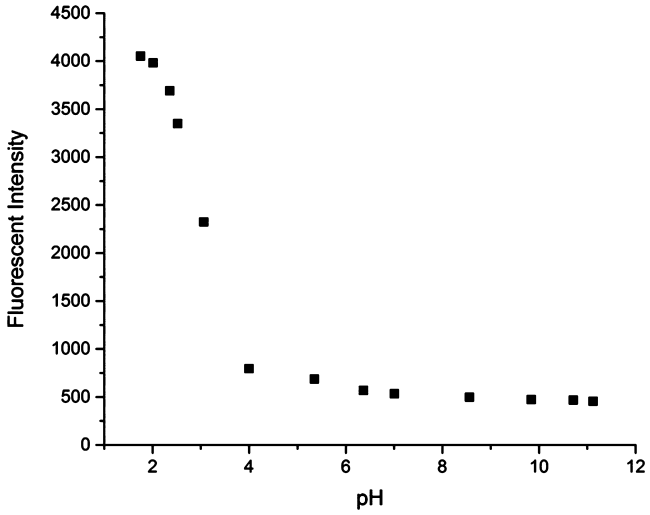

Figure 2. The fluorescence intensity at 577 nm vs. pH λ_{ex} = 560 nm.

the fluorescent pH titration (pH 1.75–11.12, λ ex = 560 nm, Figure 2) and this relationship can be quantified and fit well to the Hendersone–Hasselbach-type mass action equation $pH = pK_a + \log[(I_{max} - I)/(I - I_{min})]$.[33] According to the equation, the fluorescence intensity was linearly proportional (R^2 = 0.9884) to pH 1.70–4.00 (Figure S6), which further allows us to calculate the pH value of the sample within the range of pH from 1.75 to 4.00 based on their fluorescent intensity. The results obtained in Figure 2 are similar to the results obtained in fluorescence emission spectrum (Figure 1).

To investigate the interference of metal ions towards probe **L**, we measured the variation in the fluorescence

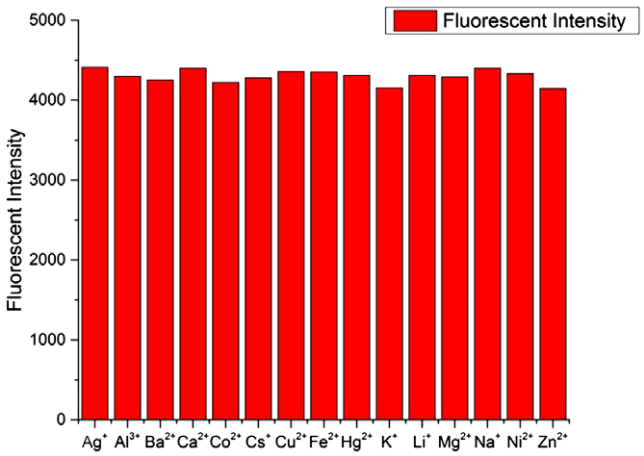

Figure 3. Fluorescence intensity changes of **L** (25 μM) at 577 nm in the presence of different metal cations in solution (B–R buffer-EtOH, v/v = 1:1) at pH 1.75.

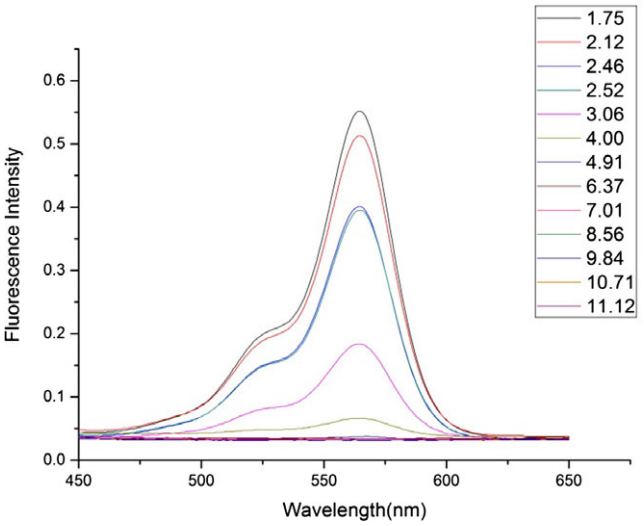

Figure 4. Absorption spectra of probe **L** (25 μM) in solution (B–R buffer-EtOH, v/v = 1:1) at various pH values.

properties of probe **L** caused by 15 ions at pH = 1.75 (Figure 3). All the co-existing ions did not show significant interfering effect on the fluorescence intensity with probe **L** even when the cations are in a much excess amount (10-fold of the probe). These results suggested that probe **L** had specific fluorescent response to acidic pH and was suitable for fluorescent intracellular pH imaging.

Further, we examined the reversibility of fluorescence vs. pH by neutralizing the solution of the probe at pH 1.75 to pH 7.01 and again acidifying it to 1.75 for circles. The probe gave high fluorescence emission intensity upon the pH value of the solution reached 1.75 and then quickly decreased to a low intensity at neutral condition in all the tested circles. As we expect, the coordination of the probe with proton is excellently reversible. In addition to that, air, light, and humidity did not show any effect on the pH-

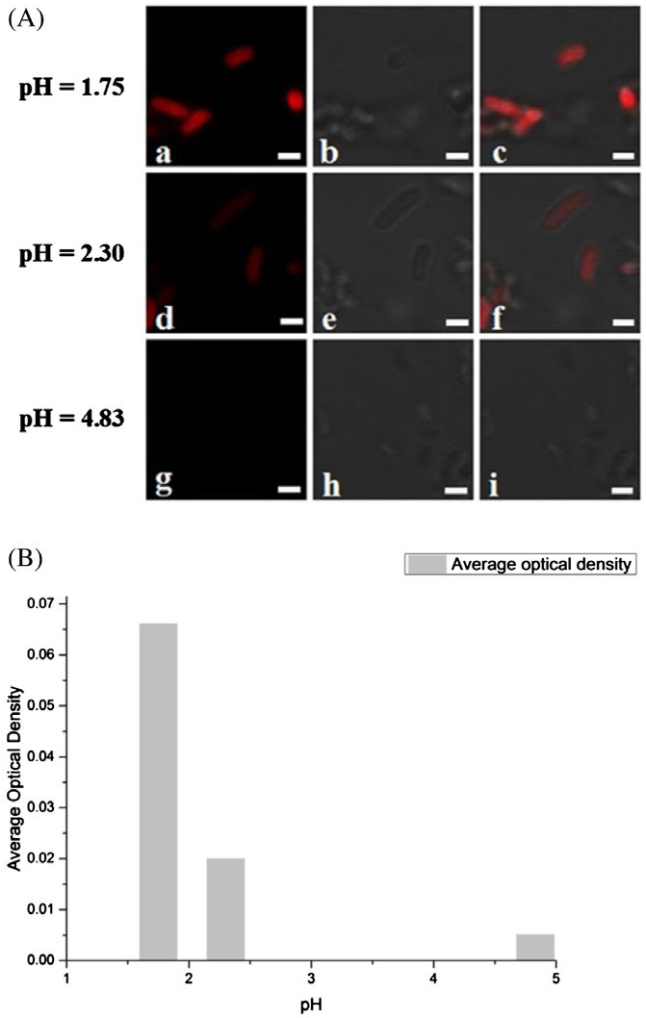

Figure 5. (A) Imaging acidity in *E. coli* cells with probe **L**. (a)–(c) pH = 1.75; (d)–(f) pH = 2.30; (g)–(i) pH = 4.83; (a), (d), and (g) are the fluorescence images; (b), (e), and (h) are the bright field; (c), (f), and (i) are merged images (scale bar: 5 μm). (B) The quantitative analysis of fluorescence intensity in *E. coli* cells.

sensing properties of probe **L** during the reversibility experiments (Figure S7). In further study on the response time of the probe, we found that probe **L** quickly gave the maximum fluorescence intensity when the pH was low at 1.75 and maintained the intensity for 20 min. The low emission intensity was given at pH 7.01 and lasted for 20 min (Figure S8).

pH Bioimaging in *E. coli*. As illustrated in Figure 4, the UV–vis absorbance intensity of probe **L** increased from pH 11.12 to 4.91, and the absorbance enhanced significantly when the pH value dropped from 4.00 to 1.75. The absorbance reached the maximum value at pH = 1.75. These results are in agreement with the tendency in fluorescence intensity, and it was further inferred that the spirolactam form existed predominantly in neutral and basic buffered media, whereas the ring-opened amide structure was formed upon acidification of the solution.

We performed the pH bioimaging of *E. coli* by a laser confocal microscope to investigate its ability to monitor the intracellular pH value. Buffers with pH at 1.75, 2.30, and 4.83 were used to incubate the bacteria. The images were captured after the probe **L** was added into above system and then washed by deionized water. Red fluorescence was clearly observed in *E. coli* under the tested acidic conditions, and the strongest fluorescence intensity was found at pH 1.75. The red fluorescence gradually disappeared when the pH decreased to 4.83, as determined by scanning confocal microscopy (Figure 5(A)), in accordance with the tendency shown in the fluorescence spectra. In addition, the quantitative analysis of fluorescence intensity in *E. coli* cells gradually increased with the drop of pH (Figure 5(B)).

Conclusion

In summary, we have developed a novel fluorescent pH probe **L** based rhodamine B by the introduction of conjugated substitution of styryl moiety to rhodamine core using coupling reaction of rhodamine hydrazine with commercially available 3-bromo-4-hydroxybenzaldehyde. The as-synthesized probe exhibit high emission intensity at 577 nm for pH 1.75, which has been confirmed its excellent selectivity and sensitivity to extremely acidic conditions. Apart from the strong selectivity, the probe has additional features like good reversibility, short response time (<1 min) and no interference with the coexisted metal ions. Moreover, this rhodamine B-based fluorescent probe may be useful for the development of colorimetric and fluorescent sensors to measure intracellular pH under extremely acidic conditions by observing fluorescence imaging of bacteria *E. coli.*

Acknowledgments. We would like to thank the Science and Technology Support Program from the Science and Technology Department of Sichuan Province China (2015FZ0070 and 2014sz0004-5), and the National Research Foundation of Korea (NRF-02016R1D1A1B01011019).

Supporting Information. Additional supporting information is available in the online version of this article.

References

1. D. -Y. Kim, H. J. Kim, *Sens. Actuators, B* **2015**, *206*, 508.
2. Z. Zhou, F. L. Gu, L. Peng, Y. Hu, Q. M. Wang, *Chem. Commun.* **2015**, *51*, 12060.
3. Z. H. Pan, G. G. Luo, J. W. Zhou, J. X. Xia, K. Fang, R. B. Wu, *Dalton Trans.* **2014**, *43*, 8499.
4. J. Qi, D. Y. Liu, X. Y. Liu, S. Q. Guan, F. L. Shi, H. X. Chang, H. R. He, G. M. Yang, *Anal. Chem.* **2015**, *87*, 5897.
5. A. K. Dengler, R. M. Wightman, G. S. McCarty, *Anal. Chem.* **2015**, *87*, 10556.
6. M. Y. Wu, K. Li, Y. H. Liu, K. K. Yu, Y. M. Xie, X. D. Zhou, X. Q. Yu, *Biomaterials* **2015**, *53*, 669.

7. S. Wiktorowski, E. Daltrozzo, A. Zumbusch, *RSC Adv.* **2015**, *5*, 29420.
8. U. C. Saha, K. Dhara, B. Chattopadhyay, S. K. Mandal, S. Mondal, S. Sen, M. Mukherjee, S. V. Smaalen, P. Chattopadhyay, *Org. Lett.* **2011**, *13*, 4510.
9. M. J. Liu, Z. Q. Ye, C. L. Xin, J. L. Yuan, *Anal. Chim. Acta* **2013**, *761*, 149.
10. Y. H. Li, Y. J. Wang, S. Yang, Y. R. Zhao, L. Yuan, J. Zheng, R. H. Yang, *Anal. Chem.* **2015**, *87*, 2495.
11. E. Teknikel, C. Unaleroglu, *Dyes Pigm.* **2015**, *120*, 239.
12. J. T. Zhang, M. Yang, C. Li, N. Dorh, F. Xie, F. T. Luo, A. Tiwari, H. Y. Liu, *J. Mater. Chem. B* **2015**, *3*, 2173.
13. J. Y. Han, K. Burgess, *Chem. Rev.* **2010**, *110*, 2709.
14. Z. Q. Qian, P. G. Dougherty, D. H. Pei, *Chem. Commun.* **2015**, *51*, 2162.
15. R. Akbar, M. Baral, B. K. Kanungo, *RSC Adv.* **2015**, *5*, 16207.
16. Z. Liu, C. N. Peng, C. X. Guo, Y. Y. Zhao, X. F. Yang, M. S. Pei, G. Y. Zhang, *Tetrahedron* **2015**, *7*, 2736.
17. H. J. Kim, C. H. Heo, H. M. Kim, *J. Am. Chem. Soc.* **2013**, *135*, 17969.
18. R. Hosseinzadeh, M. Mohadjerani, M. Pooryousef, A. Eslami, S. Emami, *Spectrochim. Acta, Part A* **2015**, *144*, 53.
19. E. Z. Wang, Y. Zhou, Q. Huang, L. Pang, H. Qiao, F. Yu, B. Gao, J. Zhang, Y. Min, T. Ma, *Spectrochim. Acta, Part A* **2016**, *152*, 327.
20. J. L. Fan, C. Y. Lin, H. L. Li, P. Zhan, J. Y. Wang, S. Cui, M. M. Hu, G. H. Cheng, X. J. Peng, *Dyes Pigm.* **2013**, *99*, 620.
21. M. Y. Yang, Y. Q. Song, M. Zhang, S. X. Lin, Z. Y. Hao, Y. Liang, D. M. Zhang, P. R. Chen, *Angew. Chem. Int. Ed.* **2012**, *51*, 7674.
22. Q. A. Best, C. J. Liu, P. D. van Hoveln, M. E. McCarroll, C. N. Scott, *J. Org. Chem.* **2013**, *78*, 10134.
23. Y. Q. Tan, J. C. Yu, J. K. Gao, Y. J. Cui, Z. Y. Wang, Y. Yang, G. D. Qian, *RSC Adv.* **2013**, *3*, 4872.
24. L. J. Liu, P. Guo, L. Chai, Q. Shi, B. H. Xu, J. P. Yuan, X. G. Wang, X. F. Shi, W. Q. Zhang, *Sens. Actuators, B* **2014**, *194*, 498.
25. S. L. Shen, X. P. Chen, X. F. Zhang, J. Y. Miao, B. X. Zhao, *J. Mater. Chem. B* **2015**, *3*, 919.
26. M. Z. Tian, X. J. Peng, J. L. Fang, J. Y. Wang, S. G. Sun, *Dyes Pigm.* **2012**, *95*, 112.
27. J. L. Tan, M. X. Zhang, F. Zhang, T. T. Yang, Y. Liu, Z. B. Li, H. Zuo, *Spectrochim. Acta, Part A* **2015**, *140*, 489.
28. T. Hasegawa, Y. Kondo, Y. Koizumi, T. Sugiyama, A. Takeda, S. Ito, F. Hamada, *Bioorg. Med. Chem.* **2009**, *17*, 6015.
29. Q. -J. Ma, H. -P. Li, F. Yang, J. Zhang, X. -F. Wu, Y. Bai, X. -F. Li, *Sens. Actuators, B* **2012**, *166*, 68.
30. Y. Xu, Z. Jiang, Y. Xiao, F. Z. Bi, J. Y. Miao, B. X. Zhao, *Anal. Chim. Acta* **2014**, *820*, 146.
31. H. S. Lv, S. Y. Huang, B. X. Zhao, J. Y. Miao, *Anal. Chim. Acta* **2013**, *788*, 177.
32. X. F. Zhang, T. Zhang, S. L. Shen, J. Y. Miao, B. X. Zhao, *RSC Adv.* **2015**, *5*, 49115.
33. F. Ge, H. Ye, J. Z. Luo, S. Wang, Y. J. Sun, B. X. Zhao, J. Y. Miao, *Sens. Actuators, B* **2013**, *181*, 15.

